Measurement of the transmission of the atmosphere from 0.2 to 2 THz

Yihong Yang, Alisha Shutler, and D. Grischkowsky*

School of Electrical and Computer Engineering, Oklahoma State University, Stillwater, Oklahoma 74078, USA
**daniel.grischkowsky@okstate.edu*

Abstract: The attenuation of electromagnetic wave propagation in the clear atmosphere from low frequencies up to 2 THz is mainly caused by water vapor. Although there have been many numerical simulations and excellent early sub-mm and far-infrared measurements of this attenuation, there has remained controversy about the background absorption in the most promising windows of transparency below 1 THz. Here, we report an accurate terahertz time-domain spectroscopy (THz-TDS) characterization of water vapor from 0.2 to 2 THz. Our results agree with the previous predicted and measured attenuations for the weak water lines, but show more attenuation for the relatively transparent windows between these lines.

OCIS codes: (010.1320) Atmospheric transmission; (010.1030) Absorption; (300.6495) Spectroscopy, terahertz.

References and links

1. A., Deepak, T.D. Wilkerson, and L. H. Ruhnke, eds., *Atmospheric Water Vapor* (Academic Press, 1980). This book is the Proceedings of the International Workshop on Atmospheric Water Vapor, Vail, Colorado, September 11–13, 1979.
2. P. H. Siegel, "Terahertz technology," IEEE Trans. Microw. Theory Tech. **50**(3), 910–928 (2002).
3. R. Appleby, and H. B. Wallace, "Standoff detection of weapons and contraband in the 100 GHz to 1 THz region," IEEE Trans. Antenn. Propag. **55**(11), 2944–2956 (2007).
4. D. E. Burch, and D. A. Gryvnak, "Continuum Absorption by Water Vapor in the infrared and Millimeter Regions," in Proceedings of the International Workshop on Atmospheric Water Vapor, Vail, Colorado, September 11–13, (1979), pp. 47–76
5. Yu. A. Dryagin, A. G. Kislyakov, L. M. Kukin, A. I. Naumov, and L. E. Fedosyev, "Measurement of the atmospheric absorption of radio waves in the range 1.36-3.0 mm," Izv. Vyssh. Uchebn. Zaved., Radiofiz. **9**, 627–644 (1966).
6. R. L. Frenkel, and D. Woods, "The microwave absorption by H2O vapor and its mixtures with other gases between 100 and 300 Gc/s," Proc. IEEE **54**(4), 498–505 (1966).
7. A. W. Straiton, and C. W. Tolbert, "Anomalies in the Absorption of Radio Waves by Atmospheric Gases," Proc. IRE **48**, 898–903 (1960).
8. V. Ya. Ryadov, and N. I. Furashov, "Investigation of the spectrum of radiowave absorption by atmospheric water vapor in the 1.15 to 1.5 mm range," Radio Phys. Quantum Electron. **15**(10), 1124–1128 (1972).
9. D. E. Burch, D. A. Gryvnak, and R. R. Patty, "Absorption of infrared radiation by CO_2 and H_2O. experimental techniques," J. Opt. Soc. Am. **57**(7), 885–895 (1967).
10. D. E. Burch, "Absorption of infrared radiant energy by CO_2 and H_2O. III. absorption by H_2O between 0.5 and 36 cm^{-1}," J. Opt. Soc. Am. **58**(10), 1383–1394 (1968).
11. M. Exter, C. Fattinger, and D. Grischkowsky, "Terahertz time-domain spectroscopy of water vapor," Opt. Lett. **14**(20), 1128–1130 (1989).
12. M. van Exter, and D. Grischkowsky, "Characterization of an optoelectronic terahertz beam system," IEEE Trans. Microw. Theory Tech. **38**(11), 1684–1691 (1990).
13. D. Grischkowsky, S. Keiding, M. Exter, and C. Fattinger, "Far-infrared time-domain spectroscopy with terahertz beams of dielectrics and demiconductors," J. Opt. Soc. Am. B **7**(10), 2006–2015 (1990).
14. T. Yuan, H. B. Liu, J. Z. Xu, F. Al-Douseri, Y. Hu, and X.-C. Zhang, "Terahertz time-domain spectroscopy of the atmosphere with different humidity," Proc. SPIE **5070**, 28–37 (2003).
15. S. Wohnsiedler, M. Theuer, M. Herrmann, S. Islam, J. Jonuscheit, R. Beigang, and F. Hase, "Simulation and experiment of terahertz stand-off detection," Proc. SPIE **7215**, 72150H, 72150H-8 (2009).
16. H.-B. Liu, H. Zhong, N. Karpowicz, Y. Chen, and X.-C. Zhang, "Terahertz spectroscopy and imaging for defense and security applications," Proc. IEEE **95**(8), 1514–1527 (2007).

#142266 - $15.00 USD Received 4 Feb 2011; revised 4 Apr 2011; accepted 16 Apr 2011; published 21 Apr 2011

1. Introduction

The absorption of THz electromagnetic radiation by water vapor controls the propagation of THz waves in the atmosphere. All considered technical, commercial and research applications of THz radiation depend on the variable amount of water vapor. The absolute humidity changes strongly with the daily weather, changing seasons, altitude and geographical location. Many simulation codes have been developed to model the absorption of THz radiation by water vapor in the atmosphere [1–3], and two examples are shown in Figs. 1 and 2. Figure 1 shows the enormous variation of THz power attenuation (dB/km) over the frequency range from 100 GHz (0.1 THz) to 1000 GHz (1 THz). The attenuation changes by 5 orders of magnitude from maximum to minimum over this frequency range. Curve A in Fig. 1. is the sum of the calculated attenuation of all the water rotational lines, plus the much weaker continuum attenuation shown as curve B, which is considered to be due to water dimers, higher-order clusters, and self-broadening of the strong water lines [4]. The attenuation due to the water lines increases linearly with the number density of water vapor, while continuum attenuation increases as the square of the number density. Consequently, the relative proportion of the total absorption due to the continuum increases linearly with the number density.

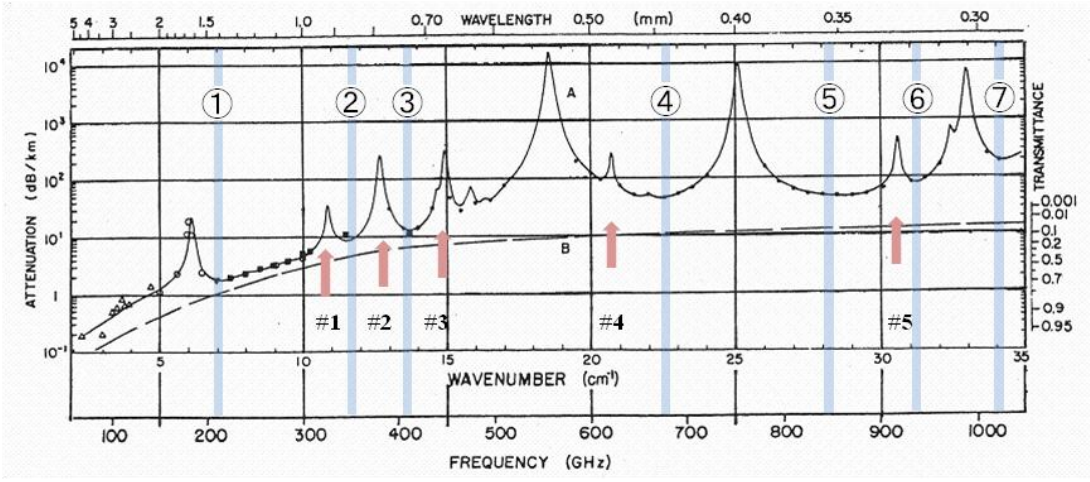

Fig. 1. This figure is a revised version of Fig. 10 of [4]. "Spectral plots of the near-millimeter attenuation by the atmospheric H_2O at sea level. H_2O density = 5.9 g/m^3. Curve A represents attenuation calculated by summing the theoretical contributions by all the lines and adding the continuum represented by curve B." [4]. The H_2O density corresponds to a relative humidity of 34% at 20 °C. The indicated measurements have been done by several groups; the open triangles below 150 GHz are from Dryagin et al. [5]; the open circles below 200 GHz are from Frenkel and Woods [6]; the filled triangle at 200 GHz is from Straiton and Tolbert [7]; the filled squares from 200 to 400 GHz are from Ryadov and Furashov [8], and the solid circles from below 400 GHz to 1000 GHz are from Burch [9,10]. 7 water windows (circled numbers) and 5 weak water lines (broad arrows) are marked for comparison with the THz-TDS measurements.

Figure 2 is an evolved and later rendition of Fig. 1 with the addition of seasonal temperature and humidity changes and the effects of fog, dust and rain. The corresponding attenuation changes by approximately 60 times (in the exponent) due to weather and seasonal changes in the water number density. The small attenuation of the water continuum is not included in Fig. 2.

Of most interest for applications are the regions (windows) of relative transparency between the absorption resonance peaks. In the windows of transparency indicated in Figs. 1 and 2, the absorption is determined by the far wings of the resonance lines, continuum absorption of the dimers, and perhaps higher clusters, all of which are not entirely understood.

#142266 - $15.00 USD Received 4 Feb 2011; revised 4 Apr 2011; accepted 16 Apr 2011; published 21 Apr 2011

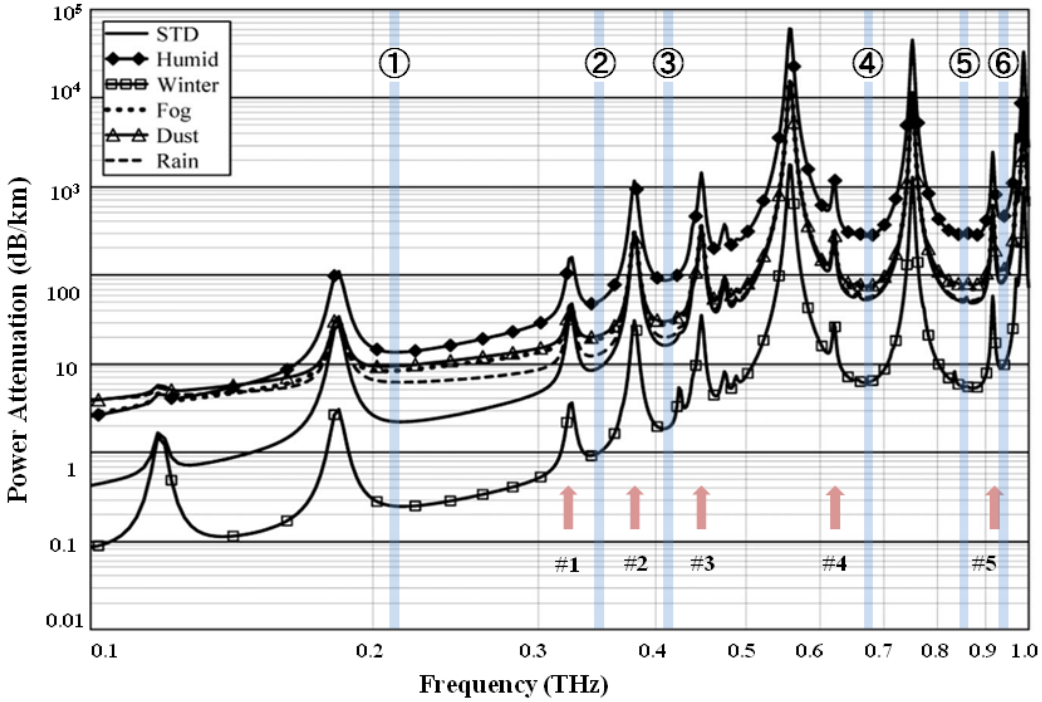

Fig. 2. Atmospheric attenuation at sea level for different conditions of temperature, relative humidity (RH), fog, dust and rain. (STD: 20 °C, RH 44%), (Humid: 35 °C, RH 90%), (Winter: –10 °C, RH 30%), (Fog, Dust, and Rain: 20 °C, RH 44%). Revised figure taken from Ref. 2. Six water windows (circled numbers) and 5 weak water lines (broad arrows) are marked for comparison with the THz-TDS measurements.

For windows 1-3 the attenuation due to the molecular water vapor and the water continuum are about the same. This ratio changes as the number density increases. Accurate measurements of attenuation with an accuracy of better than ± 1 dB/km for these regions are needed, and are difficult to achieve with laboratory sized propagation paths.

The early high quality work is well detailed in the workshop proceedings of Ref. 1, which includes both theoretical and experimental investigations of water vapor in the atmosphere. Figure 1 is a revised version of Fig. 10 of [4] showing the measured and calculated attenuation from 100 to 1000 GHz of atmospheric water vapor with a density of 5.9 g/m^3, corresponding to a relative humidity of 34% at 20 °C. The indicated measurements have been done by several groups [5–10], and their impressive accuracy presents a challenge to the recently developed optoelectronic, coherent, high-signal-to-noise technique of terahertz time-domain spectroscopy (THz-TDS) [11–13].

Previous short-path terahertz time-domain spectroscopy (THz-TDS) measurements have characterized the strong rotational lines of the water vapor spectrum [11,14], and thereby identified the transparent window regions [11,14]. A recent THz-TDS measurement of the amplitude transmission of a 1 m long atmospheric path provides meaningful results from 1 to 3 THz [15]. There has been a significant demonstration of broad-band THz pulse transmission through the ground level atmosphere for the record long-path of 108 m [16], although most of the observed low frequency attenuation was due to the frequency dependent power transfer losses in the optical train involving more than 30 mirrors.

2. Experimental setup

Here, we present a 6.18 m long-path THz-TDS measurement of the amplitude transmission of the atmosphere with a corresponding accuracy of better than ± 10 dB/km from 0.2 to 2 THz

#142266 - $15.00 USD Received 4 Feb 2011; revised 4 Apr 2011; accepted 16 Apr 2011; published 21 Apr 2011

for power transmission, which can be compared to numerical calculations, and can be used to predict long-path attenuation. The experimental set-up shown in Fig. 3 is based on the conversion of a standard THz-TDS system [11–13] to long tube operation, by removable output and input coupling mirrors. The THz-TDS system together with the removable mirrors is contained in the air-tight box #1, which is always filled with dry air. The 15 cm diameter window connecting boxes #1 and #2 is made by stretching 12.5 μm cling wrap over the opening and sealing the edges with tape. This highly transparent window is easy to make and has very little reflection at THz frequencies. Box #2 is air-tight and is connected to a 6 inch (15.24 cm) internal diameter, commercially available PVC pipe. This pipe encloses the air-tight THz path from box #2 to the 6 inch (15.24 cm) diameter, concave, spherical end mirror with a 120 inch (304.8 cm) radius of curvature. The total path length from the 6 inch end mirror to the air-tight plastic film window is 309 cm, giving the round-trip sample distance of 618 cm.

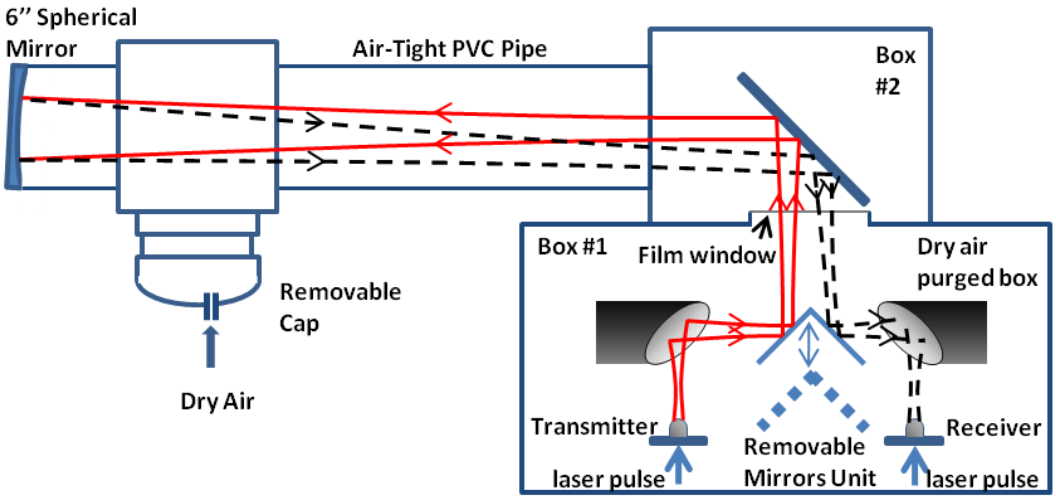

Fig. 3. Enclosed THz-TDS system for atmospheric measurements.

Including the 25 cm distance from the film window to the top of the coupling mirror prism in box #1, the total extra round trip path distance is 668 cm. This distance is chosen to equal 2 round-trips of the ultrafast optical pulses in the mode locked Ti-Sapphire pumping laser with a repetition rate of 89.82 MHz, corresponding to a round-trip distance of 334 cm. Consequently, the laser sampling pulses, used to measure the THz reference and sample pulses, are delayed by 2 pulses down the pulse train from the excitation pulses. 10 mW laser beams pumped the THz transmitter and the THz receiver. For the best THz coupling efficiency, the center of curvature of the 6 inch end mirror would be located at the THz beam waist of the THz-TDS system in box #1. However, for our case this would require the distance of 305 cm from the 6 inch end mirror to the apex of the coupling prism, instead of the 334 cm distance used for our synchronous delay. As will be described, our coupling with 334 cm is still quite acceptable.

The THz beam path from the transmitter to the 6 inch concave end mirror and back to the receiver is completely enclosed in the air-tight boxes #1 and #2 and the PVC pipe. Box #1 is always filled with dry air. Box #2 together with the PVC pipe enclosure can be filled with dry air via the connection on the PVC cap on the T connection. To make the room air measurement the cap is removed and the top of box #2 is also removed. The system is then purged with a fan at the cap opening. After equilibrium with laboratory air is obtained, the fan is turned off, and the measurements are made.

The measurement sequence is as follows: Firstly, system operation and stability are checked by measuring performance of the THz-TDS system in box #1 with the coupling mirrors removed. Secondly, the coupling mirrors are re-installed in box #1, which is then

#142266 - $15.00 USD Received 4 Feb 2011; revised 4 Apr 2011; accepted 16 Apr 2011; published 21 Apr 2011

refilled with dry air, as well as box #2 and the PVC pipe system. Then, the THz reference pulses, transmitted through the entire system filled with dry air, are measured. Thirdly, the THz sample pulses, transmitted through the PVC pipe system with the cap removed and box #2 open to laboratory humid air and with box #1 filled with dry air, are measured. Then, again the reference pulses are measured. This sequence is repeated several times during the complete transmission measurement.

3. Result and discussion

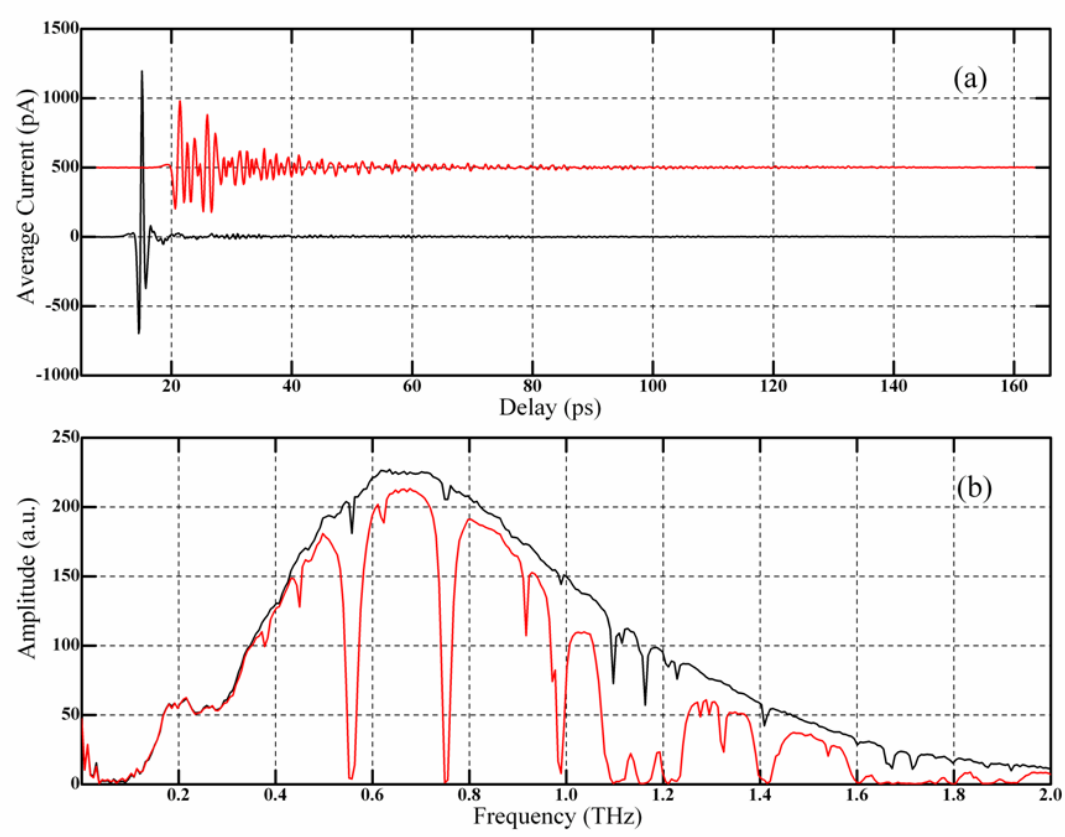

Fig. 4. (a). Measured THz reference pulse (lower trace) and measured THz sample pulse (upper trace). For clarity the THz sample pulse was shifted upwards by 500 pa. (b). Corresponding amplitude spectrum (upper curve) for the THz reference pulse and the amplitude spectrum for the sample pulse.

As shown in Fig. 4, the reference and sample pulses are measured over one scan duration of 165 ps, corresponding to the frequency resolution of 6.1 GHz. A scan consists of 625 channels (data points) with 40 μm steps between channels, corresponding to the double pass (80 μm) time step of 0.2667 ps between channels. A single scan takes 180 seconds. For a complete experimental measurement series, 4 reference dry-air pulses and 4 sample humid-air pulses were measured. Depending on the system stability and measurement conditions, several complete measurement series were performed during an experimental run. Figure 4a compares the averaged reference pulse to the averaged sample pulse. The reference pulse appears quite clean with little oscillation due to the small amount of water vapor remaining in the sample space. The sample pulse shows very strong and extended ringing from the rotational lines of water vapor, when the sample space is filled with laboratory air with 51% relative humidity at 21 °C.

#142266 - $15.00 USD Received 4 Feb 2011; revised 4 Apr 2011; accepted 16 Apr 2011; published 21 Apr 2011

During the later data analysis, the individual reference and sample pulses were zero-padded to a total scan length of 1650 ps. The amplitude spectra of these zero-padded pulses were obtained from their complex Fourier transforms and were then averaged to obtain the final amplitude spectra. The comparison of the averaged reference and averaged sample amplitude spectra is shown in Fig. 4b. The reference spectrum weakly shows the strong water lines, indicating that the residual water vapor in the sample space was less than 0.5% relative humidity. In contrast, the sample spectrum shows complete absorption

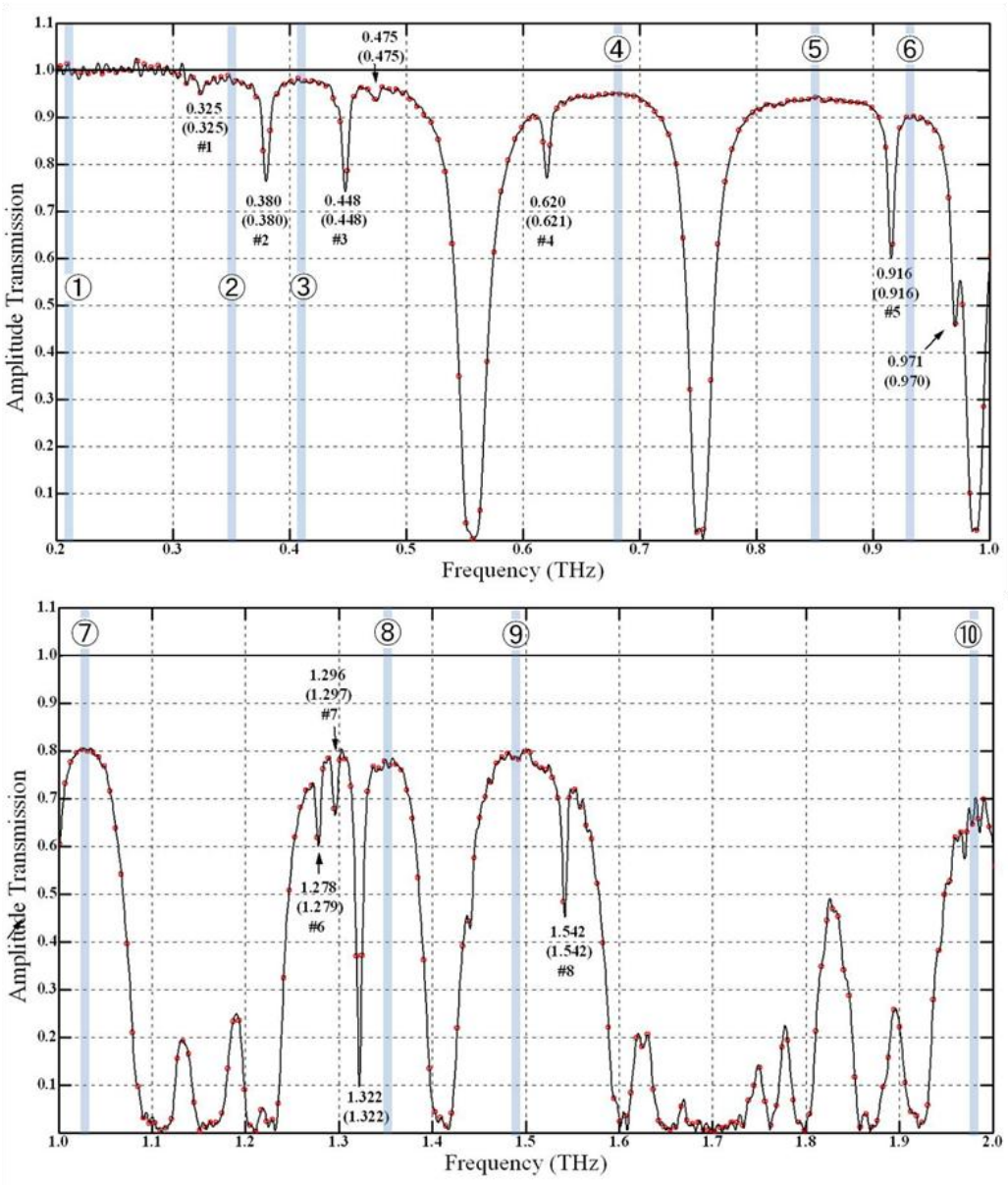

Fig. 5. The amplitude transmission through 6.18 m of atmosphere at 21 °C with RH 51%. The "real data points" are indicated by the larger open circles separated from each other by 6.1 GHz, and the interpolated points obtained from the zero-padding are separated from each other by 0.61 GHz and define the solid line. 10 water windows (circled numbers) and 8 weak water lines are marked to compare with previous predictions and measurements.

#142266 - $15.00 USD Received 4 Feb 2011; revised 4 Apr 2011; accepted 16 Apr 2011; published 21 Apr 2011

bands for the strong water lines and the significant appearance of the very weak water lines at their handbook frequencies and with resolution limited linewidths.

It is of interest to note that for the initial measurement of the THz pulse in dry box #1 with the mirrors removed, the THz pulse shape was similar to the reference pulse, but the peak extended to 3800 pa, and the corresponding peak of the amplitude spectrum at 0.65 THz had the value of 650. These numbers show that the amplitude spectral coupling from the mirror in box #1 to the 45 degree mirror in box #2 and into and through the tube to the 6 inch end mirror and then retracing the same path, but with a slight tilt to return the beam to box #1 and onto the mirror directing the beam to the THz receiver, reduces the amplitude spectrum of the reference pulse by the factor 0.35 with the corresponding factor of 0.33 for the pulse amplitude. This good coupling preserves our excellent signal to noise ratio (S/N); for the THz signal pulse, S/N = 700, while for the corresponding amplitude signal spectrum S/N = 200.

Another experimental consideration is, for the humid air case, what is the effect of a thin 100 nm layer of adsorbed water on the spherical end mirror, the outside 45 degree mirror and the outside surface of the thin plastic film window [9]. For the essentially normal incidence on the Al surfaced end mirror the total E field is zero at the surface, consequently, the water layer has negligible absorption [9]. The same situation would hold for the outside 45 degree mirror with horizontal polarization. The double pass amplitude absorption through the thin film window would be exp [– (200nm x 200/cm/2)] = 0.2%, for which the power THz absorption coefficient of liquid water was assumed to be 200/cm. For vertical polarization this attenuation would be doubled, due to the absorption by the layer on the 45 degree mirror.

The amplitude transmission shown in Fig. 5 is simply the ratio of the sample spectrum to the reference spectrum of Fig. 4b. For this result the "real data points" are indicated by the larger open circles separated from each other by 6.1 GHz, and the interpolated points obtained from the zero-padding are separated from each other by 0.61 GHz and define the solid line. The amplitude transmission maxima of the 10 windows between the weak and strong water lines decreases monotonically from the first window to No.2 (98% at 0.35 THz), to No.3 (97.5% at 0.41 THz), to No.4 (95% at 0.68 THz), to No.5 (94% at 0.85 THz), to No.6 (90% at 0.94 THz), to No.7 (80% at 1.03 THz), to No.8 (77.5% at 1.35 THz), to No.9 (79% at 1.49 THz), and to No.10 (66% at 1.98 THz). The weaker water lines appear with their expected frequencies, strengths and with linewidths equal to the spectral resolution of 6.1 GHz. The central frequency of the measured water lines is determined to an accuracy of ± 1 GHz as indicated on Fig. 5. The frequency in parenthesis is the accepted handbook value. Only water lines are observed.

The main experimental problem is maintaining the stability of the entire system, including the ultrafast laser pulseshape, repetition rate, and power in the THz pumping and THz sampling beams, the generated THz pulseshapes, bandwidth and power, coupling into and out of the sample tube and the reproducibility of the sample RH and temperature. Consequently, the best measure of the accuracy of our measurements is their reproducibility. In order to estimate our measurement accuracy, we compared the results of Fig. 5 with 2 similar independent measurements, made with completely different sets of individual pulses. The three sets of measurement data points agreed with each other to ± 1% from 0.2 to 0.4 THz; in the window regions from 0.4 to 1.0 THz these 3 transmission measurements agreed with each other to ± 0.5%, and in the windows from 1.2 to 2.0 THz, these 3 transmission measurements agreed with each other to ± 1%. We consider these results to represent our measurement accuracy and to indicate that in the first transparent window from 0.2 to 0.3 THz, the attenuation is less than 1% (equivalent to 14 dB/km for power attenuation).

Our results are summarized and compared with the previous measurements and calculations of Fig. 1 and Fig. 2 (STD: 20°C, RH 44%) in Tables 1 and 2. The values for Figs. 1-2 indicated by the asterisk have been adjusted to be directly comparable to our measurements at 21 °C with a relative humidity of 51%. Figure 1 displays the total absorption as the sum of the two contributions, curve A (the water vapor absorption) and curve B (the continuum absorption, considered to be mainly due to water dimers). The absorption due to water vapor increases linearly with the number density of water (absolute humidity), while the

#142266 - $15.00 USD Received 4 Feb 2011; revised 4 Apr 2011; accepted 16 Apr 2011; published 21 Apr 2011

absorption due to the water dimers increases as the square of the number density (absolute humidity). Figure 2 only displays the absorption due to water vapor.

Consequently, for Fig. 1, the values of (curve A - B) for the water molecules were multiplied by the factor 0.51/0.34 = 1.5, and the values of curve B for the water dimers were multiplied by the factor $(1.5)^2$. The sums of these two values are presented as Fig. 1* in both Tables. For Fig. 2, comparable values were simply obtained by multiplication by the factor (0.51/0.44) = 1.16. The resulting values are presented as Fig. 2* in both Tables.

Table 1. Comparison of Power Attenuation (dB/km) of Water Windows Shown in Fig. 1 and Fig. 2 (STD-Curve) with Experimental Results of Fig. 5Humidity for Fig. 1 is 34% and Fig. 2 is 44%.

Window (THz)	① 0.21	② 0.35	③ 0.41	④ 0.68	⑤ 0.85	⑥ 0.93	⑦ 1.03	⑧ 1.35	⑨ 1.49	⑩ 1.98
Fig. 1	2	8	12	42	45	80	180	-	-	-
Fig. 1*	(3.8)	(15.4)	(22.9)	(70.5)	(75.1)	(128)	(278)	-	-	-
Fig. 2	2.1	9.0	16	52	49	80	-	-	-	-
Fig. 2*	(2.4)	(10.4)	(18.4)	(60)	(57)	(92)	-	-	-	-
Experiment	< 7	21	28	72	92	148	314	349	314	584

* Humidity adjusted to 51% (in parenthesis) for comparison to experiment.
For window 1 experimental result indicates that the power attenuation is less than 14 dB/km.

The comparison of our water window measurements with the adjusted values of Figs. 1* and 2* to correspond to our relative humidity of 51% at 21 °C is presented in Table 1. Our results are consistently higher than for both Figs. 1* and 2*. They are in better agreement with Fig. 1*, which includes the attenuation of the continuum. We consider our disagreement to be mainly due to the broad band continuum absorption due to dimers, higher order clusters and the far-wing self broadening of the strong water lines.

Table 2. Comparison of Power Attenuation (dB/km) of Weak Water Absorption Lines Shown in Fig. 1 and Fig. 2 (STD-Curve), with Experimental Results of Fig. 5

Water Line (THz)	#1 0.325	#2 0.380	#3 0.448	#4 0.620	#5 0.916	#6 1.278	#7 1.296	#8 1.542
Figure 1	35	250	300	250	500	-	-	-
Figure 1*	(55)	(380)	(455)	(385)	(760)	-	-	-
Figure 2	50	300	360	310	600	-	-	-
Figure 2*	(58)	(345)	(415)	(355)	(690)	-	-	-
Experiment	72	380	420	365	720	720	575	1115

Humidity for Fig. 1 is 34% and Fig. 2 is 44%.
* Humidity adjusted to 51% (in parenthesis) for comparison to experiment.

Our measurements are in much better agreement for the strengths of the weak water lines as shown in Table 2. Here, the results of Figs. 1* and 2* are in better agreement with each other and our measurements are consistent with both. In terms of fractional error, our measurements from 0.2 to 1.0 THz, the water line strengths are more precise than for the water windows, because the total absorption for the lines was between 23% to 40%, while that for the windows was only between 0.5% to 10%. Consequently, for precisely measuring, the most transparent water windows 1-3, a humidity controlled path length of 60m would be required to obtain total absorptions between 1% to 25%.

4. Summary

This high resolution measurement provides the most accurate THz-TDS results to date for the transmission windows and the absorption strengths of the weak lines of the water vapor transmission of the atmosphere. This accuracy and sensitivity shows promise for THz monitoring of the atmosphere for pollutants and dangerous gases. These THz-TDS measurements were compared with the much earlier, high-quality sub-mm and far-infrared FTS measurements. The THz-TDS measured power attenuations for the 7 windows between 0.2 and 1 THz were significantly higher than the earlier work, while the THz-TDS measured

#142266 - $15.00 USD Received 4 Feb 2011; revised 4 Apr 2011; accepted 16 Apr 2011; published 21 Apr 2011

attenuation for the 5 weak water lines between 0.2 and 1.1 THz were in relatively good agreement. The window disagreement is considered to be due in part to the variability of the broad background continuum absorption in the atmosphere. However, the measured window transparency is acceptable for short-range ranging, communications and imaging applications.

Acknowledgments

We acknowledge careful readings of this manuscript by Joseph S. Melinger, and particularly thank him for bringing Ref. 1 to our attention. This work was partially supported by the DTRA (10-2960M), the Air Force Research Laboratory (AFRL) and the National Science Foundation.

#142266 - $15.00 USD Received 4 Feb 2011; revised 4 Apr 2011; accepted 16 Apr 2011; published 21 Apr 2011